

Rocky Mountain Society of Artificial Intelligence. Third Annual Rocky Mountain Conference on Artificial Intelligence. Denver, Colorado. 1988.

Scarlato, Panagiotis D. Knowledge-Based Systems for Water Resources Management. South Florida Water Management District. West Palm Beach, Florida. 1988.

Simons & Associates, Inc. Expert System for the Operation of the Mark Twain Reservoir System. Project prepared for the U.S. Army Corps of Engineers, St. Louis District. Fort Collins, Colorado. 1989.

U.S. Army Corps of Engineers, St. Louis District. Mark Twain Lake Preliminary Water Control Manual. St. Louis, Missouri. 1984.

Waterman, Donald A. A Guide to Expert System. Addison-Wesley Publishing Company. Menlo Park, California. 1986.

Characteristic Based Finite Volume Method for the Solution of Transport Equations in Groundwater

M. Putti,¹ W. W-G Yeh,¹ W. A. Mulder²

Abstract

A finite volume method based on triangular cells is proposed for the numerical discretization of the general two-dimensional transport equation in groundwater systems. The scheme combines the flexibility of finite elements in the treatment of complex geometries and general boundary conditions with the simplicity, robustness, and efficiency peculiar of finite difference methods. High-resolution upwind schemes are adopted in order to maintain accuracy when the equation is dominated by advection. The preprocessing approach is employed: the dependent variables are first monotonically interpolated and then used for the calculation of the exact solution of the Riemann problems at the interfaces between the cells. The method is non-oscillatory and globally second order accurate in space and time. The scheme automatically introduces small amounts of numerical viscosity depending on the smoothness of the solution: when the solution is smooth enough, no numerical dissipation is visible. Numerical experiments show good agreement with analytical solutions for a full range of cell Peclet numbers.

1 Introduction

Numerous finite element and finite difference schemes have been proposed for the numerical simulation of convective-diffusive problems. Preference to the finite element method is usually given when geometrically complex domains and general boundary conditions are to be modeled. On the other hand, finite difference schemes are preferred when the equations are defined on regular domains because of their computational efficiency. However, when advection dominates the process, the application of both

¹Department of Civil Engineering, University of California, Los Angeles, CA 90024

²Department of Mathematics, University of California, Los Angeles, CA 90024

formulations requires the use of special techniques in order to damp the spurious oscillations that are introduced by the numerical scheme in the presence of sharp fronts.

The method of characteristics in conjunction with finite element and finite difference techniques (Neumann 1984, Farmer 1985) (mixed Eulerian Lagrangian formulations) has been used as a technique to reduce oscillatory behavior at sharp fronts. Discontinuities are tracked throughout the domain using Lagrangian techniques, while the dispersive fluxes are solved using Eulerian formulations. The resulting scheme is accurate but computationally expensive and non-conservative.

Alternatively Eulerian formulations encompassing both the dispersive and the advective terms offer greater efficiency, but with the result that numerical solutions often display either spurious oscillations or fronts that are not as steep as expected (Richtmeyer and Morton 1967, Sun and Yeh 1983, Wang and Yeh 1986). To damp the non-physical oscillations, upwind and upstream weighted schemes are commonly used for both finite difference and finite element methods. This is achieved at the expense of accuracy: it can be proven that a scheme which is strictly non-oscillatory cannot be of order of accuracy greater than one (Roe 1986).

Van Leer (1977) introduced upwind schemes which are second order accurate almost everywhere. Since then, a family of 'high resolution shock capturing' schemes has been developed which combine non-oscillatory properties and global high order of accuracy (Chakravarthy and Osher 1985, van Leer 1985). The idea that enables these schemes to be oscillation-free and accurate, is interpreting the numerical scheme as a description of an integral rather than a differential equation, thus allowing the presence of discontinuities. Finite volumes techniques naturally arise as substitutes for finite differences. Second order of accuracy is achieved by utilizing solutions to local Riemann problems (Godunov-type schemes (Godunov 1959)) as follows: first the concept of 'monotone interpolation' is used to automatically change the dependent variables when non-oscillatory criteria are violated, and then the theory of characteristics is used to locally solve pure advective problems at the interfaces between control volumes. Extensions of these schemes to more than one spatial dimension are usually based on the solution of local Riemann problems along directions that are orthogonal to the faces of the control volumes.

Chakravarthy and Osher (1985) describe a method for the implementation of such schemes on triangular control volumes, over which the dependent variables are integrated. This finite volume technique is used and extended in the present research. The scheme is applied to the advective-dispersive equation governing the motion of contaminants in groundwater systems. Because of its definition on generally shaped triangular elements, the procedure is particularly attractive for these problems. It combines the flexibility in the description of complex geometries and general boundary conditions characteristic of finite element methods with the computational efficiency and accuracy achievable by 'high resolution shock capturing' fi-

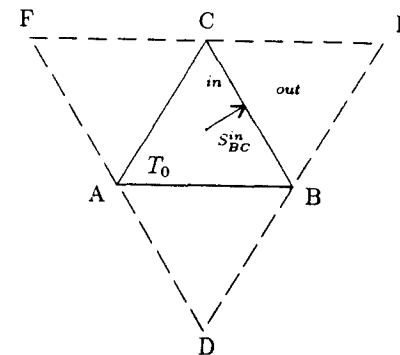


Figure 1: Triangular Control Volumes: Notations for the Derivation of the Discrete Convective and Dispersive Fluxes

nite difference discretizations.

2 The Finite Volume Approach

The finite volume approach is based on discrete representation of the dependent variable as volume integral averages. The derivation of the numerical scheme will be done using the following general model problem for the contaminant transport equation in groundwater:

$$\frac{\partial c}{\partial t} + \nabla \cdot \mathbf{F} = \nabla \cdot \mathbf{D} \nabla c \quad (1)$$

where c is the concentration of the contaminant in the water, ∇ is the gradient operator, and $\mathbf{F} = \mathbf{v} c$ is the vector flux. The derivation is carried out over triangular control volumes as shown in figure 1.

After integration over the triangle ABC, interchanging the time-derivative and the space integration operators, equation 1 can be rewritten as:

$$\begin{aligned} \frac{\partial}{\partial t} c_{ABC} &= \frac{1}{A_{T_0}} \left[- \int_{T_0} \nabla \cdot \mathbf{F} d\mathbf{x} + \int_{T_0} \nabla \cdot \mathbf{D} \nabla c d\mathbf{x} \right] \\ c_{ABC} &= \frac{1}{A_{T_0}} \int_{T_0} c d\mathbf{x} \end{aligned} \quad (2)$$

The variable c_{ABC} will be the new dependent variable that will be used in the numerical formulation. Application of the divergence theorem to the preceding equation, gives:

$$\frac{\partial}{\partial t} c_{ABC} = -\frac{1}{A_{T_0}} \cdot \left\{ \left[\int_{T_0} \mathbf{F} \cdot \hat{\mathbf{n}}_{AB} ds + \int_{T_0} \mathbf{F} \cdot \hat{\mathbf{n}}_{BC} ds + \int_{T_0} \mathbf{F} \cdot \hat{\mathbf{n}}_{CA} ds \right] - \left[\int_{T_0} D\nabla c|_{AB} \cdot \hat{\mathbf{n}}_{AB} ds + \int_{T_0} D\nabla c|_{BC} \cdot \hat{\mathbf{n}}_{BC} ds + \int_{T_0} D\nabla c|_{CA} \cdot \hat{\mathbf{n}}_{CA} ds \right] \right\} \quad (3)$$

where:

$\mathbf{F}_{AB}, \mathbf{F}_{BC}, \mathbf{F}_{CA}$ are the convective fluxes along the sides of triangle T_0 ,

$D\nabla c|_{AB}, D\nabla c|_{BC}, D\nabla c|_{CA}$ are the dispersive fluxes,

$\hat{\mathbf{n}}_{AB}, \hat{\mathbf{n}}_{BC}, \hat{\mathbf{n}}_{CA}$ are the unit outward normal vectors for each side of T_0 .

The semi-discrete version of the preceding equation for the triangle under consideration can be written as:

$$\frac{\partial}{\partial t} c_{ABC} = \frac{1}{A_{T_0}} \left\{ -[\hat{f}_{AB} + \hat{f}_{BC} + \hat{f}_{CA}] + [\hat{D}_{AB} + \hat{D}_{BC} + \hat{D}_{CA}] \right\} \quad (4)$$

where \hat{f} and \hat{D} are the space discretizations of the convective fluxes and of the dispersive fluxes across the sides of T_0 respectively.

2.1 Discretization of Convective Fluxes

The convective numerical flux across side BC can be written as:

$$\hat{f}_{BC} = \mathbf{n}_{BC} f(\tilde{c}_{BC}^{in}, \tilde{c}_{BC}^{out}) \quad (5)$$

where $f(\cdot, \cdot)$ is a Riemann problem solver. The superscripts "in" and "out" refer to quantities calculated just inside and just outside of triangle T_0 across side BC. In the present linear case equation 5 can be written as:

$$\hat{f}_{BC} = \begin{cases} \tilde{c}_{BC}^{in} \mathbf{v}_{ABC}^{in} \cdot \mathbf{n}_{BC} & \text{if } \mathbf{v}_{ABC}^{in} > 0 \\ \tilde{c}_{BC}^{out} \mathbf{v}_{ABC}^{out} \cdot \mathbf{n}_{BC} & \text{if } \mathbf{v}_{ABC}^{in} < 0 \end{cases} \quad (6)$$

This corresponds to the solution of a Riemann problem across side BC, assuming all coefficients to be constants in the two neighboring control volumes.

The value of \tilde{c} is calculated so that second order accuracy is achieved. Define the differences

$$\begin{aligned} \alpha_{AB} &= c_{AB}^{out} - c_{AB}^{in} \\ \alpha_{BC} &= c_{BC}^{out} - c_{BC}^{in} \\ \alpha_{CA} &= c_{CA}^{out} - c_{CA}^{in} \end{aligned} \quad (7)$$

and let

$$\left(\frac{\partial c}{\partial n} \right)_{BC}^{in} = \frac{\minmod[\overline{BC}\alpha_{BC}, \overline{AB}\alpha_{AB}\hat{\mathbf{n}}_{AB} \cdot \hat{\mathbf{n}}_{BC} + \overline{CA}\alpha_{CA}\hat{\mathbf{n}}_{CA} \cdot \hat{\mathbf{n}}_{BC}]}{A_{T_0}} \quad (8)$$

where:

$$\minmod(x, y) = \text{sign}(x) \cdot \max\{0, \min[|x|, y \text{sign}(x)]\} \quad (9)$$

Then \tilde{c}_{BC}^{in} is written as the value of c averaged over T_0 and ascribed to the centroid, but transferred to the side BC and limited by e.g. 9:

$$\tilde{c}_{BC}^{in} = c_{ABC} + s_{BC}^{in} \left(\frac{\partial c}{\partial n} \right)_{BC}^{in} \quad (10)$$

where s_{BC}^{in} is the distance between the side BC and the centroid of T_0 . Note that: $\tilde{c}_{BC}^{out} = \tilde{c}_{CB}^{in}$, that is the value of \tilde{c} outside T_0 through side BC is computed as the value of \tilde{c} inside T_1 , contiguous to T_0 through side CB.

This formulation introduces small amount of first order numerical viscosity only when the solution front is steep. In this manner the scheme does not produce numerical oscillations when the solution is discontinuous, and adds second order artificial viscosity in smooth regions of the solution. Any other flux limiter beside 'minmod' can be employed (Roe 1986).

2.2 Discretization of the Dispersive Flux

The dispersive fluxes on triangle T_0 are represented by the second term of the right hand side of equations 3 and 4. For each side of the control volume a normal derivative, $\partial c / \partial n$, and a tangential derivative $\partial c / \partial s$, can be defined. For example for side BC in figure 1, the normal derivative can be discretized as:

$$\left(\frac{\partial c}{\partial n} \right)_{BC} = \frac{c_1 - c_0}{b_1 b_0} \quad (11)$$

The tangential derivatives can be approximated numerically using areal averages at the vertices of the control volume:

$$\begin{aligned} \bar{c}_B &= \frac{1}{\sum_{i=1}^{N_B} A_{T_i}} \sum_{i=1}^{N_B} A_{T_i} c_i \\ \bar{c}_C &= \frac{1}{\sum_{j=1}^{N_C} A_{T_j}} \sum_{j=1}^{N_C} A_{T_j} c_j \end{aligned}$$

where N_B and N_C are the numbers of elements sharing respectively node B and node C, and c_i and c_j are the averaged values on such triangle. Then the tangential derivative can be written as:

$$\left(\frac{\partial c}{\partial s} \right)_{BC} = \frac{\bar{c}_B - \bar{c}_C}{\overline{BC}} \quad (12)$$

The derivatives along the coordinate axes : $(\partial c/\partial x)_{BC}$ and $(\partial c/\partial y)_{BC}$, can be easily evaluated by projections.

The dispersive flux in equation 4 for side BC can be approximated by:

$$\widehat{D}_{BC} = D \widehat{\nabla c}|_{BC} \cdot \mathbf{n}_{BC} \overline{BC} \quad (13)$$

where:

$$D \widehat{\nabla c}|_{BC} = \left[\left(\frac{\partial c}{\partial x} \right)_{BC}, \left(\frac{\partial c}{\partial y} \right)_{BC} \right]^T$$

This is a consistent approximation to the dispersive flux for equation 1. Actually, as will be described in section 3, it has been shown numerically to be a second order accurate discretization, as long as the triangulation does not become too irregular.

2.3 The Time-Discretization

For the discretization of the time-dependent part of the equation, Hancock's scheme has been employed (van Albada 1982). This technique is a two-step explicit scheme that can be shown to be second order accurate. Denoting by $\widehat{F} = \widehat{f} - \widehat{D}$ the total flux (convective and dispersive) the scheme can be written as:

$$\begin{aligned} c^{n+\frac{1}{2}} &= c^n - \frac{1}{2} \Delta t \widehat{F}^*(c^n) \\ c^{n+1} &= c^n - \Delta t \widehat{F}(c^{n+\frac{1}{2}}) \end{aligned}$$

where the superscript n denotes the time-stage ($0 \leq n \leq N$) and Δt the time-step so that $T = N \Delta t$. In the first step $\widehat{F}^* = \widehat{f}^* - \widehat{D}$ the asterisk denotes that the convective flux is calculated using values inside the control volume interpolated from the centroid to the boundary of the cell. No Riemann problems are solved in this step and this makes the scheme more efficient than the usual two-step second order accurate technique.

3 Numerical Experiments

A one-dimensional problem has been simulated on a two-dimensional grid. The domain is represented by a rectangle with unit length and small width to enable preservation of one-dimensional flow characteristics. All the examples were carried out using two different triangulations of the domain, with equilateral and rectangular triangles (figure 2a,b). No differences are visible in the numerical solutions calculated on the two different grids.

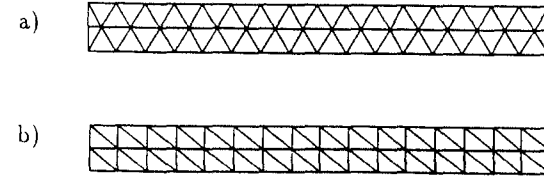


Figure 2: Triangulations Used for the Numerical Experiments: a) Equilateral Triangles. b) Rectangular Triangles.

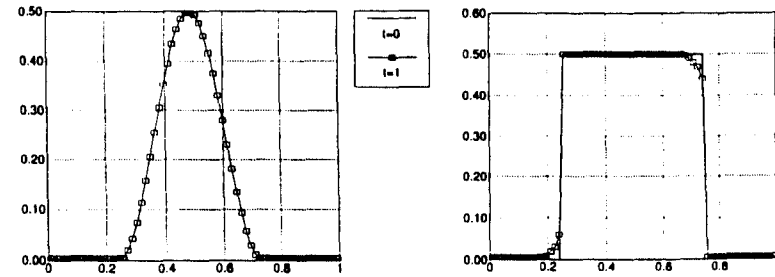


Figure 3: Purely Hyperbolic Example. Concentrations for $h=1/64$: a) \sin^2 -Wave and b) Square-Wave

3.1 Purely Hyperbolic Case

To test the non-oscillatory behavior and the accuracy of the scheme at the sharp fronts, a pure hyperbolic equation is solved with constant unitary velocity and periodic boundary conditions. Two different initial conditions are considered in the experiments: a smooth \sin^2 -wave and a discontinuous square wave.

Results indicate the scheme performs quite satisfactorily. The numerical solution never displays oscillations, validating the theoretical results that the scheme is TVD. Small amounts of artificial viscosity are visible only in the case of discontinuous initial data (fig. 3).

The asymmetry noted in the square-wave case is a consequence of the particular limiter adopted in the formulation (minmod). Other limiters may produce slightly different results which may be more or less accurate depending on the problem. The accuracy however will always remain of second order in smooth regions of the flow both in space and time. It

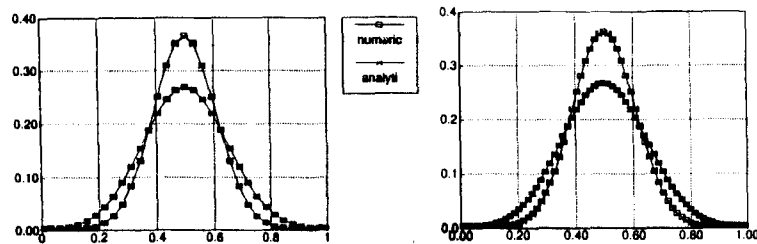


Figure 4: Purely Diffusive Example. Concentrations at a) $h=1/32$ and b) $h=1/64$

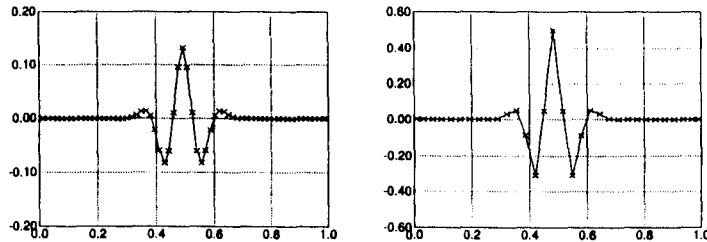


Figure 5: Purely Diffusive Example. Residuals at $t=0$: a) $h=1/32$; b) $h=1/64$

is interesting to note that the scheme reproduces the exact solutions for the examples mentioned when the CFL number is set to one, even when working on a two-dimensional grid.

3.2 Purely Diffusive Case

A pure diffusive problem with constant coefficients is solved to test the accuracy of the discretization of the second order term. The numerical and analytical solutions are plotted in figure 4 for different mesh-sizes. To determine the accuracy of the space discretization the residual at $t = 0$ is calculated. Figure 5 shows the graph of the residual vs. x . The resulting plot is of the shape of the fourth derivative of the solution, suggesting that the method is globally second order accurate in space.

To test the overall accuracy the norms of the solution errors (difference between exact and numerical solutions) and of the residuals are plotted vs.

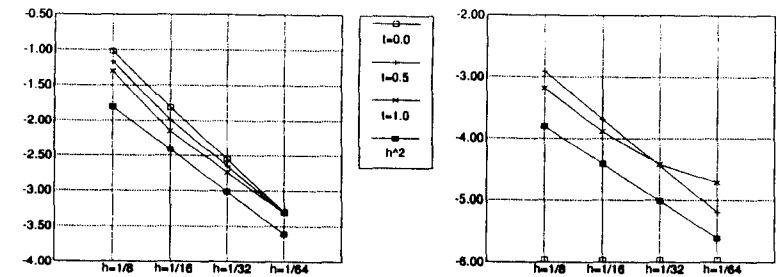


Figure 6: Purely Diffusive Example. Natural Logarithm of the Norms of: a) Residuals, and b) Solution Errors. Compared with the h^2 -Line.

the cell-size (figure 6). The results show that both the norms of the errors and of the residuals are described by functions that decrease quadratically as the mesh-size decreases. This implies that the overall accuracy of the finite volume formulation is second order.

3.3 Comparison with MCB approach of Sun and Yeh

The last series of test has been performed on the convection-diffusion equation, whose analytical solution can be found e.f. in Bear (1979). The example is taken from Sun and Yeh (1983) so that results of the present formulation can be compared with those of the Multiple Cell Balance (MCB) finite element approach. The simulation was performed with three different sets of coefficients:

- a) $v=1$, $D=10$, which gives $Pe=0.5$;
- b) $v=1$, $D=0.05$, which gives $Pe=100$;
- c) $v=1$, $D=5 \times 10^{-5}$, which gives $Pe=10000$.

The results are plotted in figures 7 and 8. They show a good agreement with the analytical solution for a wide range of Peclet numbers. Comparisons with the MCB finite element approach suggest that the two methods are more or less equivalent when the Peclet number is small. However when the Peclet number increases the finite volume approach becomes more accurate, introducing smaller amounts of numerical viscosity. This can be easily seen by evaluating the width of the front for the analytical solution and for the numerical solutions obtained with the two methods (table 1).

4 Conclusions and Future Research

Results from numerical experiments, suggest that the finite volume approach, together with high resolution upwind scheme, is a promising technique for the solution of the transport equations in groundwater contamination problems. The solutions obtained show that the method is second order accurate in space and time: numerical calculations compare very favorably with analytical expressions for a full range of Peclet numbers. The triangular shape of the control volumes allows great flexibility in handling complex geometries and is well suited for localized mesh refinements. The finite volume approach is very simple as compared to the finite element method and allows for the use of high resolution upwind schemes to treat steep fronts. All these factors make the technique efficient as far as the space discretization is concerned.

Ongoing research includes testing of the scheme with more challenging two-dimensional problems, with eventual application directed toward the solution of the coupled equations describing multiphase flow. Also the possibility of improving the efficiency of the scheme by means for example of implicit time-stepping techniques could be explored. The method in fact should give rise to system matrices that are reasonably well-conditioned and suitable to be solved numerically (van Leer and Mulder 1985).

Acknowledgments

The work was supported in part by the Toxic Substances Research and Teaching Program, University of California, Davis.

References

- [1] Bear, J. *Hydraulics of Groundwater* McGraw Hill, New York, 1979.
- [2] Chakravarthy S. and S. Osher. Computing with high Resolution: Upwind Schemes for Hyperbolic Equations. *Lectures in Applied Mathematics*, 22:57-86, 1985.
- [3] Farmer C. L. Moving Point Techniques. In *Fundamentals of Transport Phenomena in Porous Media*, Proceedings of the NATO Advanced Study Institute, Newark, Delaware, 1985.
- [4] Godunov S. K. Finite Difference Method for Numerical Computation of Discontinuous Solution of the Equation of Fluid Dynamics. *Mat. Sbornik*, 47:357-393, 1959.

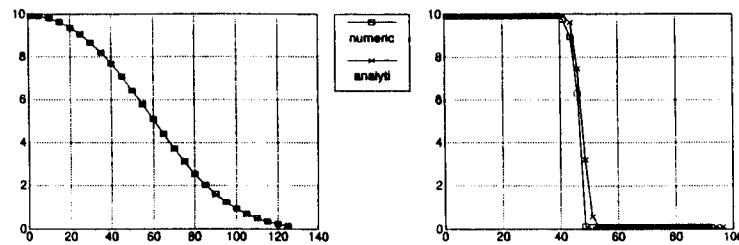


Figure 7: Convective-Dispersive Example. a) $Pe=0.5$, b) $Pe=50$

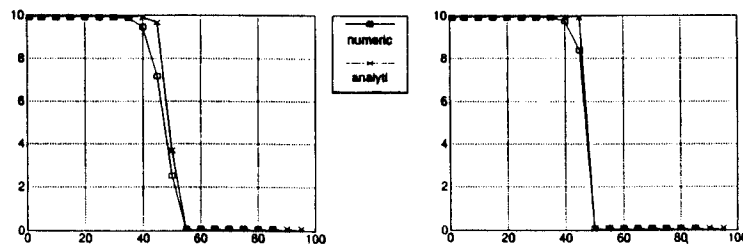


Figure 8: Convective-Dispersive Example. a) $Pe=100$, b) $Pe=10000$

	analytic solution	finite volume	MCB finite element
width of front (m)	15	20	30

Table 1: Width of the Front in the Case $Pe=100$: Comparison among Different Solutions

Characteristics of the Flow of a Gravity Well in a Crossflow

1 2
Hosam M. Moghazi, James K. White
and Helmi S. Hathoot 3

ABSTRACT

Using the finite element method, a three dimensional model has been designed to study the characteristics of flow near a gravity well in a steady crossflow. The effects of the vertical velocity near the well and the height of the seepage face have been studied. Previous studies by others did not take into consideration these factors. Determination of the height of the seepage face, the discharge, the position of the stagnation point and the corresponding head in terms of the drawdown in the well and the initial slope of the groundwater are made and all are presented graphically in chart forms suitable for practical use.

INTRODUCTION

A fundamental assumption on which the behaviour of the flow toward a pumping well is based is that the initial water table is horizontal and hence that no movement of groundwater exists prior to the time that the well is pumped. Such a condition is not generally found in nature especially in the case of steep crossflow, where the area of influence surrounding a gravity well is not circular and the water particles take a more circuitous path as shown in figure 1.

Only analytical studies have been made to investigate this problem, based on the Dupuit assumptions (1863) where the vertical velocity near the well was neglected. Therefore an inaccurate position of the free surface near the well is

¹Department of Civil Engineering, Kings College London, University of London, London, Strand WC2R

²LS, U.K.

Department of Civil Engineering, Kings College London, University of London, London, Strand WC2R 2LS, U.K.

³Department of Irrigation and Hydraulic, Faculty of Engineering, Alexandria University, EGYPT.

- [5] Neumann S. P. Adaptive Eulerian-Lagrangean Finite Element Method for Advection-Dispersion. In *International Journal for Numerical Methods in Engineering*, 20:321-337, 1984.
- [6] Richtmeyer R. D. and K. W. Morton. *Difference Methods for Initial-Value Problems*. Interscience, New York, 1967.
- [7] Roe P. L. Some Contributions to the Modelling of Discontinuous Flows. *Lectures in Applied Mathematics*, 22:163-193, 1985.
- [8] Roe P. L. Characteristic-Based Schemes for the Euler Equation. *Annual Review of Fluid Dynamics*, 18:337-365, 1986.
- [9] Sun N-Z. and W. W-G. Yeh. A Proposed Upstream Weight Numerical Method for Simulating Pollutant Transport in Groundwater. *Water Resources Research*, 19(6):1489-1500, 1983.
- [10] Sweby P. K. High Resolution Schemes Using Flux Limiters for Hyperbolic Conservation Laws. *SIAM Journal of Numerical Analysis*, 21:995-1011, 1984.
- [11] van Albada, G. D., and B. van Leer, and W. W. Roberts Jr. A Comparative Study of Computational Methods in Cosmic Gas Dynamics, *Astronomy and Astrophysics*, 108:76-86, 1982.
- [12] van Leer B. Towards the Ultimate Conservative Difference Scheme. III: Upstream Centered Finite Difference Schemes for Ideal Compressible Flow. *Journal of Computational Physics*, 23:263-275, 1977.
- [13] van Leer B. Upwind-Difference Method for Aerodynamic Problems Governed by the Euler Equation. *Lectures Notes in Applied Mathematics*, 22:327-336, 1985.
- [14] van Leer B. and W. A. Mulder. Relaxation Methods for Hyperbolic Conservation Laws. F. Angraad, A. Dervieux, J.A. Desideri, and R. Glowinski editors. *Numerical Methods for the Euler Equation of Fluid Dynamics*, SIAM, Philadelphia, 312-333, 1985.
- [15] Wang C. and W. W-G. Yeh. An Upstream Weight Multiple Cell Balance Finite-Element Method for Solving Three Dimensional Convection-Dispersion Equations. *Water Resources Research*, 22(11):1575-1589, 1986.